Case Studies in Thermal Engineering 29 (2022) 101698

Contents lists available at ScienceDirect

Case Studies in Thermal Engineering

journal homepage: www.elsevier.com/locate/csite

Thermal visualization of Ostwald-de Waele liquid in wavy trapezoidal cavity: Effect of undulation and amplitude

Hijaz Ahmad [a], Rashid Mahmood [b], Muhammad Bilal Hafeez [c,*], Afraz Hussain Majeed [b], Sameh Askar [d], Hasan Shahzad [e]

[a] International Telematic University Uninettuno, Corso Vittorio Emanuele II, 39, 00186, Roma, Italy
[b] Department of Mathematics, Air University, PAF Complex E-9, Islamabad, 44000, Pakistan
[c] Gdansk University of Technology, Faculty of Mechanical Engineering and Ship Technology, Institute of Mechanics and Machine Design, Narutowicza 11/12, 80-233, Gdańsk, Poland
[d] Department of Statistics and Operations Research, College of Science, King Saud University, P.O. Box 2455, Riyadh, 11451, Saudi Arabia
[e] Faculty of Materials and Manufacturing, College of Mechanical Engineering and Applied Electronics Technology, Beijing University of Technology, China

ARTICLE INFO

Keywords:
Mixed convection
Ostwald-de Waele fluid
Wavy trapezoidal cavity
Finite element method (FEM)
Undulation

ABSTRACT

The present study is concerned with the numerical simulations of Ostwald-de Waele fluid flow in a wavy trapezoidal cavity in the presence of a heated cylinder situated at the center of the cavity. The work consists in characterizing the mixed convection as a function of the intensity of heat flow. The flow behaviour and temperature distribution in a cavity are the main focus of this study. The lower wall of the cavity is fixed and heated while the wavy surface is insulated and moves with a constant speed. The sloping walls are kept cold and are subject to zero no-slip conditions for velocity components. The whole setup is modeled as a set of coupled partial differential equations and is solved by the Finite Element Method. For pressure and velocity approximations, we use the stable finite element pair $\mathbb{P}_2 - \mathbb{P}_1$, while for temperature approximation we use the space of linear polynomial as $\mathbb{P}_1$. The ranges of the parameters involved in the study are the Ostwald-de Wale index $(0.5 \leq n \leq 1.5)$, Prandlt number $(1 \leq \mathrm{Pr} \leq 10)$, Grashof number $(100 \leq Gr \leq 1000)$, the number of undulation $(0 \leq \lambda \leq 4)$, and the non-dimensional amplitude of the wavy surface $(0.02 \leq A \leq 0.06)$. The major findings of the study are shown using velocity profile, streamlines, and isotherms. Moreover, the kinetic energy and average (Nu_{avg}) Nusselt number is determined for various values of the parameters involved.

1. Introduction

Research into mixed convection has gained a lot of attention because of its wide range of applications including building ventilation, storage of grains, chemical removal of thin films, disposing of water material, the cooling of electrical parts, etc. respectively Conventional approaches were studied extensively in ventilated enclosures. F. Penot [1] has analyzed the computational study of free convection inside the square cavity in the presence of a large Grashof number. Moreover, he examined the variation in Nusselt numbers for different inclinations. Xin et al. [2] studied the numerical effects of the partially heated air-filled cavity with a direct interpretation

* Corresponding author.
E-mail addresses: hijaz555@gmail.com (H. Ahmad), rashid.mahmood@mail.au.edu.pk (R. Mahmood), muhammad.bilal.hafeez@pg.edu.pl (M.B. Hafeez), chafrazhussain@gmail.com (A. Hussain Majeed), saskar@ksu.edu.sa (S. Askar), hasanshahzad99@hotmail.com (H. Shahzad).

https://doi.org/10.1016/j.csite.2021.101698
Received 15 September 2021; Received in revised form 20 November 2021; Accepted 5 December 2021

Available online 6 December 2021

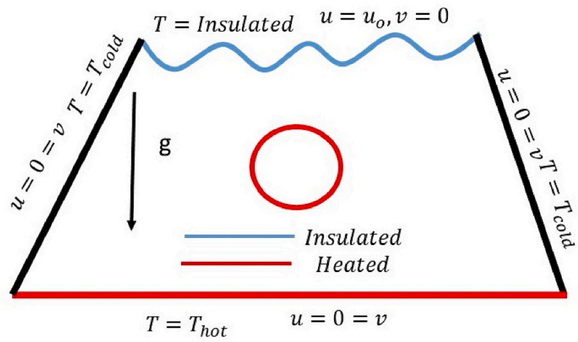

Fig. 1. The schematic diagram for the physical problem.

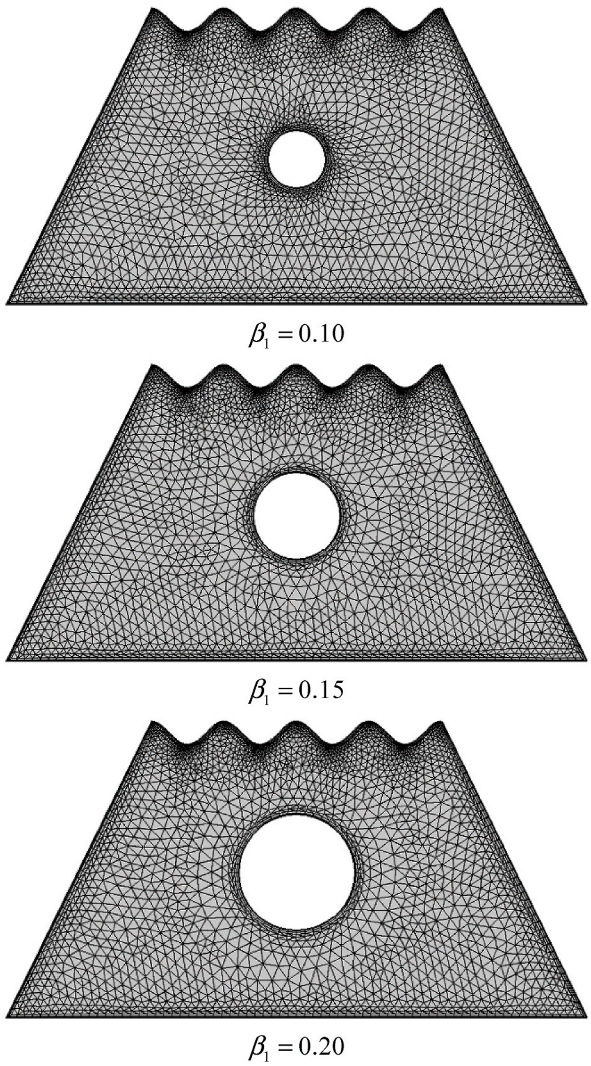

Fig. 2. A computational grid at fine level mesh for various diameters of the cylinder.

of the two-dimensional equations. They found that significant thermal performance in high *Ra*. Khanafer et al. [3] considered a numerical calculation of mixed convection heat transfer in open-ended enclosures. Also studied the average Nusselt number for different parametric values. Manca et al. [4] have investigated experimentally mixed convection in a cavity with a heated inflow wall. Also discussed is the impact of the Nusselt number in the presence of the Richardson number. Heat transfer in a gas – filled enclosure with a

Table 1
Grid convergence test for various refinement levels.

Refinement Level	Nu_{avg}
L_1	9.0371
L_2	9.8817
L_3	10.3292
L_4	11.0793
L_5	11.5317
L_6	11.9202
L_7	13.2979
L_8	14.4972
L_9	14.4972

Table 2
Mesh statistics versus different refinement levels for various diameters of the cylinder β_1.

Refinement Level	#EL	#DOF	#EL	#DOF	#EL	#DOF
L_1	530	4162	458	3694	488	3937
L_2	856	6569	776	6049	772	6071
L_3	1282	9674	1192	9089	1174	9020
L_4	2246	16516	2016	15021	1830	13860
L_5	2908	21143	2646	19488	2590	19220
L_6	4468	31799	4128	29685	4042	29270
L_7	10086	71040	10516	74123	10758	75984
L_8	39116	264919	39304	266669	39016	198540

partially heated horizontal wall and thermally insulated side walls was studied by Lin et al. [5]. Laguerre et al. [6] examined both experimental and numerical analysis of heat transfer by natural convection in a cavity filled with the cylinder. Also observed are the effects of thermal stratification and circular airflow in the cavity. Mahmoudi et al. [7] studied the numerical influence of mixed convection flow and heat transfer in a vented square cavity. Saury et al. [8] studied the characterization of a large Rayleigh number in the air-filled cavity. Furthermore, analyzed the impact of Nusselt number along both hot and cold walls. Xu et al. [9] described the unsteady thermal flow adjacent heated to the sidewall of the cavity. Yousaf et al. [10] examined the thermal and hydrodynamic behaviors were studied in a sinusoidal wavy square cavity. Chorin et al. [11] have numerically simulated the natural convection flow with thermal disturbance in the partially heated cavity. Furthermore, the local temperature variation of the hot wall affects global heat transport.

The power-law fluid is the simplest and most frequent model for non-Newtonian fluids, which has attracted a lot of attention from researchers. The important factor of this model is power-law index "n" when $n = 1$, then fluid goes to Newtonian behaviors and when $n > 1$ and $n < 1$, means that the shear thickening and thinning behaviors in the fluid. Ohta et al. [12] investigated a numerical study of the thermal effect of pseudo-plastic fluid in a square cavity. In addition, analyzing the behavior of shear-thinning on viscous fluid. Lamsaadi et al. [13] studied the heat transfer in a rectangular cavity containing power-law fluids. Moreover, analyzed to the uniform heat flux along the side walls. Barth et al. [14] analyzed the comparison of both experimental and numerical impact of benchmark problem for natural convection of Newtonian fluid in the cubical cavity. Kaddiri et al. [15] investigated thermo-dependent viscous fluid confined in a square cavity and uniformly heated lower wall by using a finite difference scheme. Turan et al. [16] studied the effect of two-dimensional laminar natural convection of non-Newtonian Ostwald-de Waele fluid in a rectangular cavity with partially heated sidewalls. Sheremet et al. [17] numerically investigated the heat transfer in right angle trapezoidal cavity filled by nano-fluid of porosity medium in the presence of Buongiorno's mathematical method. Mahmood et al. [18] studied comparison of Newtonian and non-Newtonian fluid and also for more computational results by using highly refined hybrid mesh. Mahmood et al. [19] examined the effect of shear-thickening and shear-thinning flow in a channel-driven cavity. In addition, analyzed the significant impact of drag and lift forces. Mahmood et al. [20] characterized numerically non-linear Ostwald-de Waele fluid in a channel with a square obstacle. Also studied the influence of power-law index on pressure drop.

In this study, the Ostwald de Waele fluid in a sinusoidal wavy trapezoidal cavity having circular obstacles is studied by considering the different diameters of the circle. The paper is organized as follows: In section 2 geometry of the problem and its mathematical modeling is defined. In section 3 solution to the problem is proposed. In section 4 outcomes of the problem are summed up. In the last section conclusion based on the results and discussion, a section is drawn.

2. Mathematical modelling

Considered 2-dimensional, laminar, incompressible fluid flow with uniform physical properties in a trapezoidal cavity. The obstacle and the bottom wall are considered heated while the sinusoidal upper wall is considered cold as well as insulted and the other

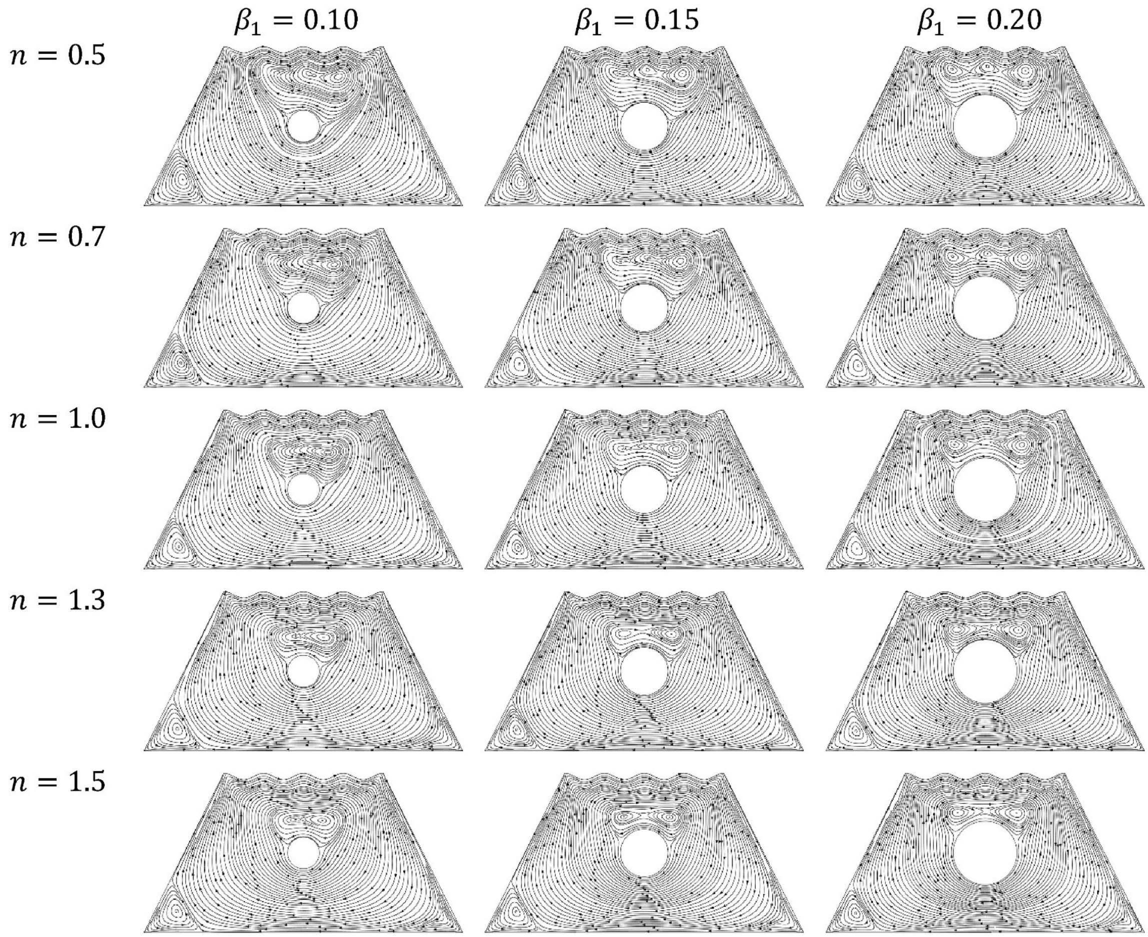

Fig. 3. Influence of n on velocity for $\mathrm{Re} = 20$, $Pr = 5$ and $Gr = 1000$.

two walls are kept cold (see Fig. 1). Introducing the set of non-dimensional variables

$$(x, y) = \frac{(X, Y)}{H}, (u, v) = \frac{(U, V)}{u_o}, \theta = \frac{T - T_{cold}}{T_{hot} - T_{cold}}, \quad p = \frac{P}{\rho u_o^2}. \tag{1}$$

where x and y are non-dimensional coordinates measure along horizontal and vertical axes, respectively.

Also u, v and θ are non-dimensional velocity and temperature. Using these non-dimensional variables in Navier Stokes equations [15] to obtain the non-dimensional governing equations

$$u_x + v_y = 0, \tag{2}$$

$$uu_x + vu_y = -p_x + \frac{1}{\mathrm{Re}}(\nabla.\boldsymbol{\tau})_X, \tag{3}$$

$$uv_x + vv_y = -p_y + \frac{1}{\mathrm{Re}}(\nabla.\boldsymbol{\tau})_Y + \frac{Gr}{\mathrm{Re}^2}\theta, \tag{4}$$

$$u\theta_x + v\theta_y = \frac{1}{\mathrm{RePr}}\left(\theta_{xx} + \theta_{yy}\right), \tag{5}$$

Where the subscript X and Y represent X and Y components of the stress tensor τ, respectively. The non-dimensionalized equations (2)–(5) suggest that pressure, velocity, and temperature dependents on non-dimensional parameters Reynolds number, Grashof number, and Prandtl number. These parameters are defined as

$$\text{Reynolds No} \quad Re = \frac{u_o L}{\upsilon}$$

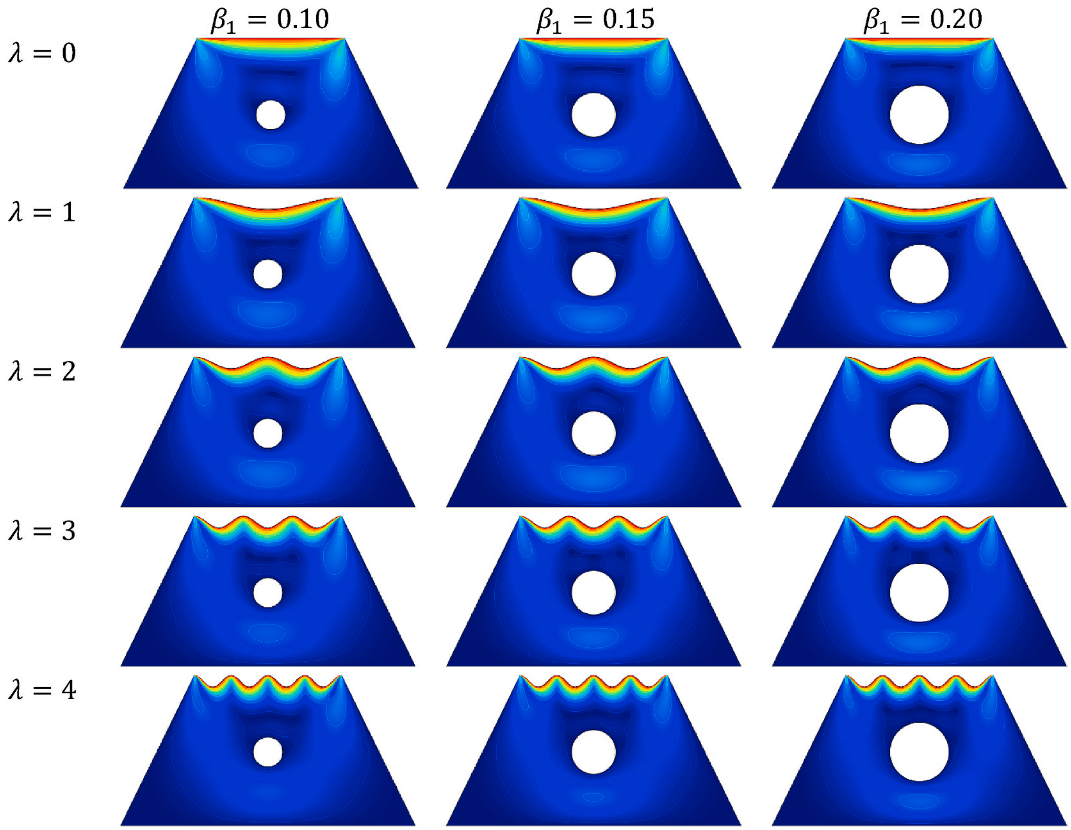

Fig. 4. Influence of λ and β_1 on velocity for Re $= 20$, $Pr = 5$ and $Gr = 1000$.

Grashof No $\quad Gr = \dfrac{g\beta(T_{hot} - T_{cold})L^3}{\upsilon^2}$

Prandtl No $\quad Pr = \dfrac{\upsilon}{\alpha}$

Where ν be the kinematic viscosity, g be the gravitational acceleration and β be the volumetric coefficient of expansion.

The lower wall of the trapezoidal cavity is fixed and uniformly heated while the wavy surface is insulated and moves with a constant speed. The sloping walls are kept cold and are subject to zero no-slip conditions for velocity components. For a generalized Newtonian fluid, which obeys the Ostwald-de Waele fluid [15] in non-dimensional Cartesian coordinate we define:

$$\boldsymbol{\tau} = m(\dot{\boldsymbol{\gamma}})^n, \tag{6}$$

The kinetic energy is a very major quantity for flow in a driven cavity which evaluates the scale of momentum for the entire flow. Kinetic energy is defined as

$$E_K = \frac{1}{2}\int_{\Omega} \langle \mathbf{u}.\mathbf{u} \rangle d\Omega. \tag{7}$$

To evaluate the characteristic of heat transfer, which is in terms of local Nusselt number is shown as $Nu_{\text{local}} = -\frac{\partial\theta}{\partial n}$, compute the average Nusselt numWber on the walls of the cavity, the heated cylinder is obtained by utilizing the following mathematical formulation

$$Nu_{avg} = \frac{1}{S}\int_{S} Nu_{\text{local}} dS. \tag{8}$$

where n and S are normal direction and the thermal region of the surface, it is reasonable to assume that the Nu_{avg} depends on the Prandlt number.

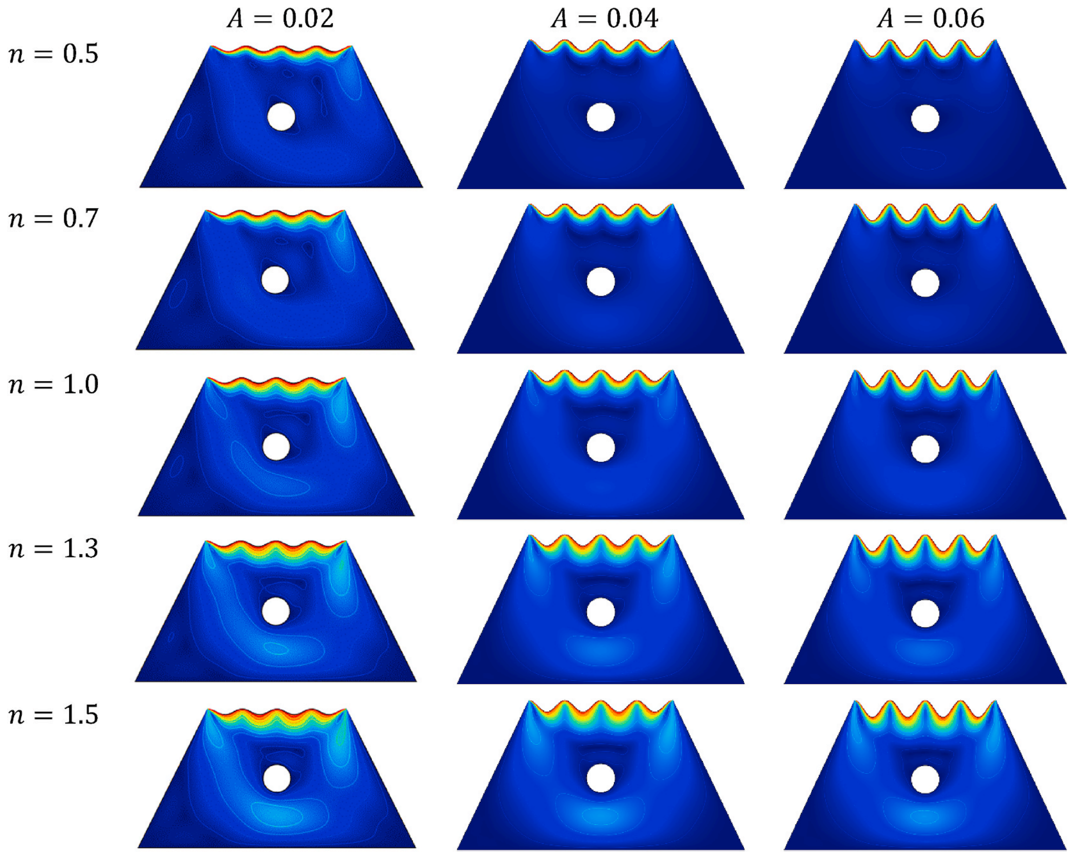

Fig. 5. Influence of n and A on velocity for $\mathrm{Re} = 20$, $Pr = 5$ and $Gr = 1000$.

3. Numerical scheme and grid convergence

The system of partial differential equations (2)–(5) cannot be solved analytically as they are nonlinear and the presence of non-Newtonian fluid in the trapezoidal wavy cavity; we used the numerical scheme FEM to compute the optimal solution with various diameters of a cylinder. The Newton method was used to solve the original discrete non-linear system of equations, and the linearized inner system was solved with the PARDISO direct solver. In order to achieve the needed level of convergence with less iterations, the PARDISO solver is used along with LU matrix factorization [21,22].

A hybrid grid is generated in the present work to capture the rapid changes in the dependent variables near the boundaries. Fig. 2 reveals the computational grids at fine level (L_6) for different diameters of the cylinder. To see the adequacy of the grid chosen for simulations, a grid independence study was performed by computing the average Nusselt number on heated surfaces as a benchmark quantity.

No noteworthy variations in Nu_{avg} were detected with grid refinement at the higher level in space are shown in Table 1. All results were simulated for parameters setting as $Pr = 5, \beta_1 = 0.10$, $n = 1$, $\lambda = 4$, and $Gr = 100$, respectively. The criteria of convergence for the non-linear iteration is set as to $\left|\frac{\psi^{i+1} - \psi^{i}}{\psi^{i+1}}\right| < 10^{-6}$, in which ψ represent the general solution component representing velocity, pressure, and temperature.

Table 2 shows the mesh statistics for the number of elements (#EL) and the related degrees of freedom (#DOF) at various refinement stages.

4. Results and discussion

The results are obtained from computations carried out in three diameters of the cylinder are present in the sinusoidal wavy trapezoidal cavity, for the several values of power-law index n, the non-dimensional parameter Reynolds number $Re = 20$ and Grashof number $Gr = 1000$ are fixed, respectively. The velocity field, streamline, velocity profile, and isotherms resulting from the calculations carried out are revealed in Fig. 3 to Fig. 7, respectively.

The impact of fluid flow in the sinusoidal wavy trapezoidal enclosure by the influence of cylinder diameter β_1 from left to right and characteristic of the power-law index from top to bottom n are examined in Fig. 3 at $\mathrm{Re} = 20$, $Gr = 1000$ and $Pr = 5$. The streamlines are presented in Fig. 3 for different values of flow behavior index (n) and various diameter size of the cylinder. Enhancement in the size

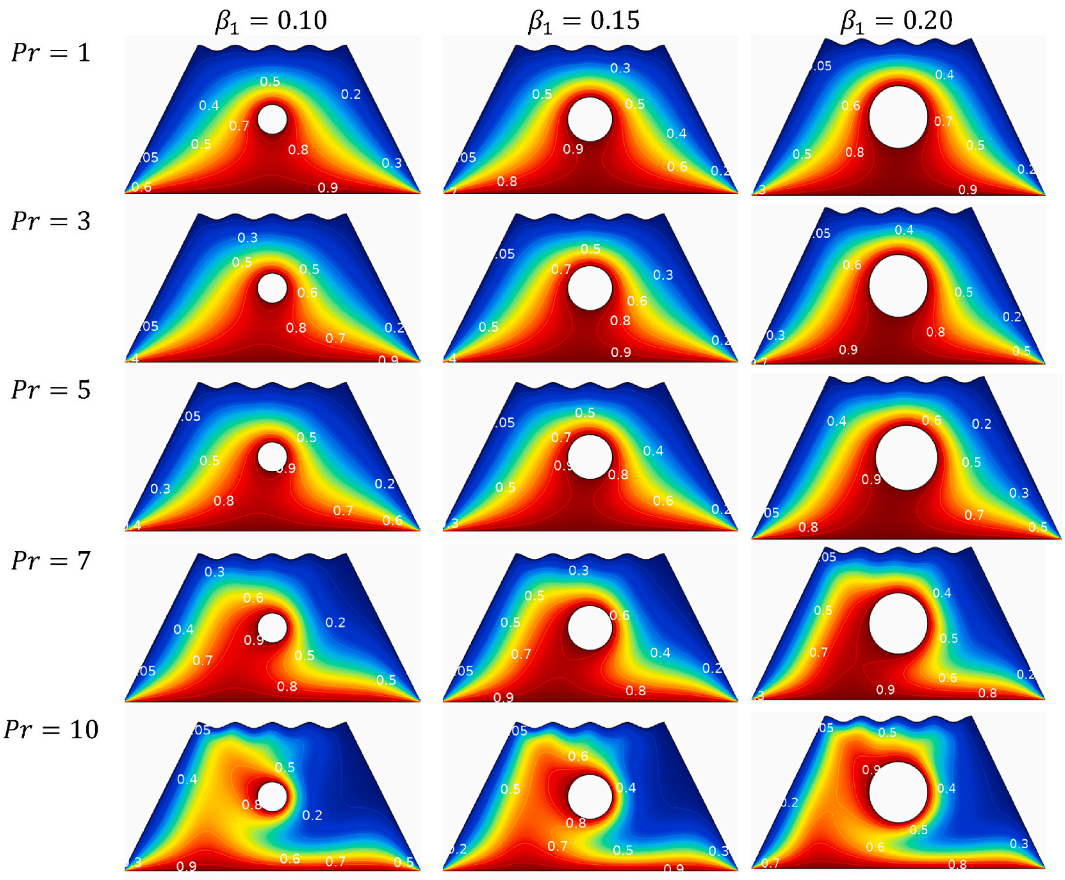

Fig. 6. Influence of Pr on isotherm for $\mathrm{Re} = 20$, $Pr = 5$ and $Gr = 1000$.

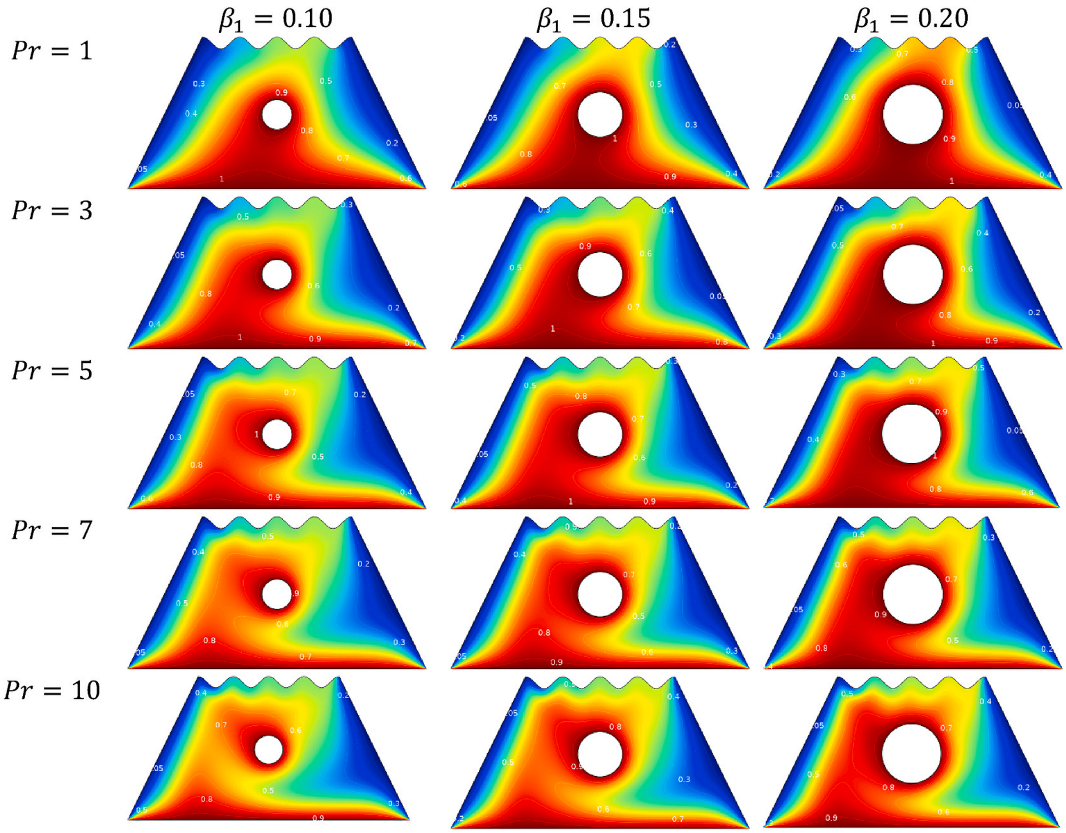

Fig. 7. Influence of *Pr* on isotherm for Re = 20, *Pr* = *5* and *Gr* = 1000.

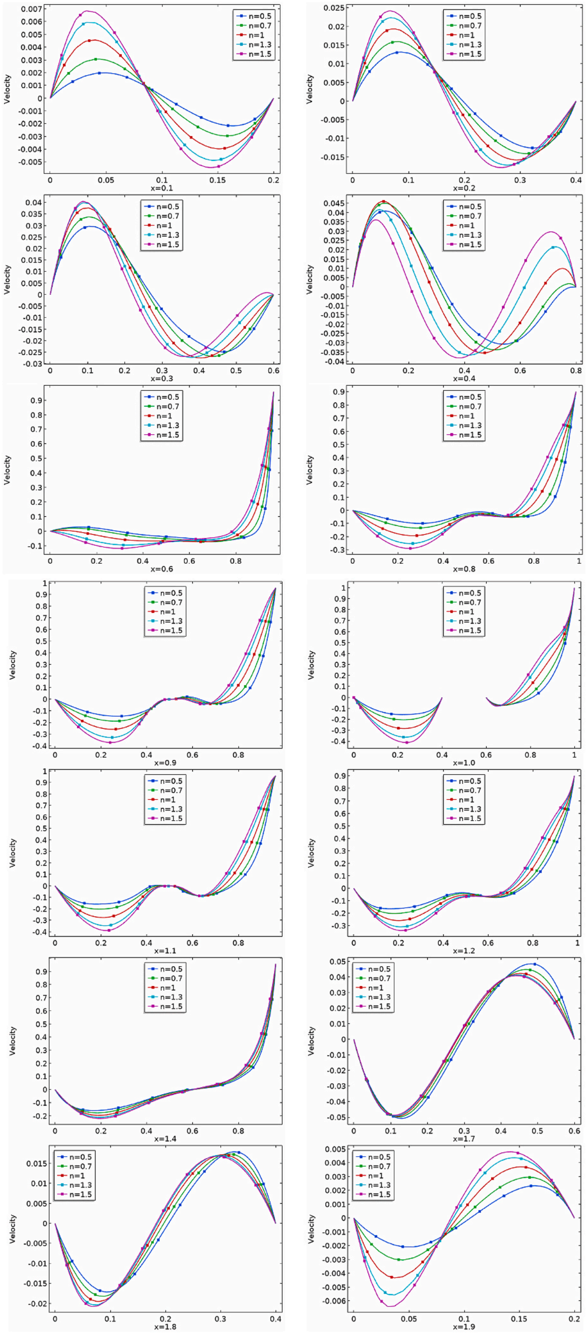

Fig. 8. Evaluation of velocity profile at different positions for various *n*.

of diameter for shear-thinning regime, three small eddies occur near the upper region of the obstacle while at the higher values of *n*, reduces the numbers of eddy on that region.

In Fig. 4, the effects of undulation on velocity profile have been revealed against different diameters of the cylinder. From these plots, it is examined that the undulation of the upper surface effect the boundary layer thickness. The velocity profile for the different amplitude of the wavy surface and various values of the Ostwald - de Waele index (*n*) are shown in Fig. 5. It can be noticed from Fig. 5

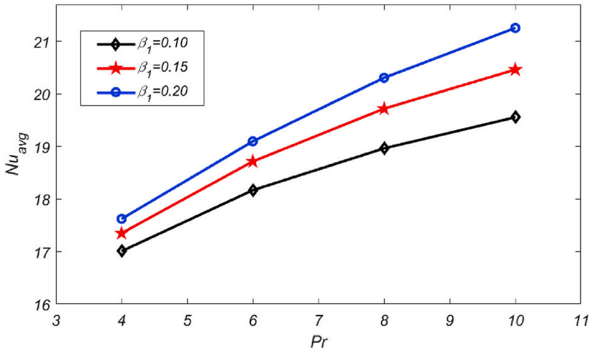

Fig. 9. Nu_{avg} versus *Pr* for different values of cylinder diameter.

Table 3
Influence on kinetic energy for different power-law exponent *n* with various diameters of cylinders β_1.

n	E_K	E_K	E_K
0.5	1.92820E-06	2.01884E-06	2.07042E-06
0.7	3.46810E-06	3.58642E-06	3.68649E-06
1.0	5.93405E-06	6.10043E-06	6.26452E-06
1.3	8.55611E-06	8.76358E-06	8.98087E-06
1.5	1.03818E-05	1.06110E-05	1.08524E-05

that the vortices clustered near the upper corners of the cavity. Moreover, the strong vortices are occurring in case of increasing *n* at the minimum amplitude of the wavy surface while enhancement of amplitude, the weak vortices appear at the corners of the wavy surface.

The corresponding isotherm contours for variations of Prandtl number *Pr* from top to bottom and several diameter sizes of the cylinder from left to right are shown in Fig. 6. Further, it was observed that the heat transfer rapidly increases for both values of *Pr* and β_1. Fig. 7 shows that the effects of insulated wavy surface on the isotherms for various *Pr* and β_1. The adiabatic wavy surface gives rise to an increased heat transfer mechanism as compared with the cold one.

All these observations are due to the strengthening of the mixed convection with the variation of Prandtl number *Pr* and several lengths of cylinder diameter are illustrated in Fig. 5 with constant Grashof number $Gr = 1000$.

For a better description, we have evaluated multiple line graphs at different *x* locations as shown in Fig. 8. They reveal that the variation in velocity is very mild on the left side of the wavy region whose line graphs are drawn at $x = 0.1$, 0.2, 0.3, and 0.4. The same behavior is observed after the wavy region at $x = 1.7$, 1.8, and 1.9. However, the strength of backflow increases in the wavy region of the cavity as is evident from the line graphs at $0.6 \leq x \leq 1.4$.

The effect of the size of the obstacle on the average Nusselt number against *Pr* is displayed in Fig. 9. This demonstrates that when we increase the *Pr* and β_1 that results in enhancement of the average Nusselt number showing more heat transfer due to an increase of the convection phenomenon. In order to determine a functional dependence of Nu_{avg} versus *Pr*, the method of least squares has been implemented for the case $\beta_1 = 0.10$. The relation turned out to be $Nu_{avg} = 14.7421 + 0.5128\, Pr$ where 14.7421turns out to be the y-intercept and 0.5128 is the slope of linear trend.

We tabulate the kinetic energy at the various power-law exponent *n* for different diameters of the cylinder shown in Table 3. We observe that the kinetic energy is increased for the increment of both power-law exponents as well as the diameter of cylinders in a sinusoidal wavy trapezoidal cavity which implies both the parameters provide a direct relation with the kinetic energy.

5. Conclusions

In this pagination, the characteristics of heat and fluid flow inside a wavy trapezoidal cavity containing a heated cylinder have been explored. Finite Element Method (FEM) is employed using mixed finite elements utilized on a hybrid-refined grid to yield highly accurate results in terms of velocity profile, streamline patterns, and isotherms. The numerical simulations have been performed against restricted ranges of parameters n, λ, A, Pr, Re and Gr to generate different convection regimes. The flow rate enhances significantly for different diameter of cylinders and uniformly heating wall. The main findings of this study include the following:

- Both the parameters *n* and β_1 provide a direct relation with the kinetic energy.
- The higher values of *n*, reduce the numbers of eddies near the wavy region.
- The strong vortices appear for increasing *n* at the minimum amplitude of the wavy surface.
- Adiabatic wavy surface gives rise to increased heat transfer mechanism as compared with the cold one.
- Number of eddies in the cavity is strongly influenced by the diameter of the obstacle as is evident from the stream function plots.
- A functional dependence of Nu_{avg} on *Pr* has been calculated using the method of least squares that suggested a linear trend.

Authorship contributions

Hijaz Ahmad: Conceptualization. Rashid Mahmood: Supervision. Muhammad Bilal Hafeez: Mathematical Modeling. Afraz Hussain Majeed: Writing original drafts. Sameh Askar: Fundings. Hasan Shahzad: Software.

Declaration of competing interest

The authors declare that they have no known competing financial interests or personal relationships that could have appeared to influence the work reported in this paper.

Acknowledgment

Research Supporting Project number (RSP-2021/167), King Saud University, Riyadh, Saudi Arabia.

References

[1] F. Penot, Numerical calculation of two-dimensional natural convection in isothermal open cavities, Numer. HeatTransfer 5 (1982) 421–437.
[2] S. Xin, P. Le Quéré, Direct numerical simulations of two-dimensional chaotic natural convection in a differentially heated cavity of aspect ratio 4, J. Fluid Mech. 304 (1995) 87–118.
[3] K. Khanafer, K. Vafai, L. Marilyn, Mixed convection heat transfer in two-dimensional open-ended enclosures, Int. J. Heat Mass Tran. 45 (2002) 5171–5190.
[4] O. Manca, S. Nardini, K. Vafai, Experimental investigation of mixed convection in a channel with an open cavity, Exp. Heat Tran. 19 (2006) 53–68, 2006.
[5] Y. Lin, B. Farouk, Heat transfer in a rectangular chamber with differentially heated horizontal walls: effects of a vibrating sidewall, Int. J. Heat Mass Tran. 51 (2008) 3179–3189.
[6] O. Laguerre, S. Benamara, D. Remy, D. Flick, Experimental and numerical study of heat and mo-isture transfers by natural convection in a cavity filled with solid obstacles, Int. J. Heat Mass Tran. 52 (2009) 5691–5700.
[7] A.H. Mahmoudi, M. Shahi, F. Talebi, Effect of inlet and outlet location on the mixed convective cooling inside the ventilated cavity subjected to an external nanofluid, Intern.Comm. in Heat and Mass Transfer 37 (2010) 1158–1173.
[8] D. Saury, N. Rouger, F. Djanna, F. Penot, Natural convection in an air-filled cavity : experimental results at large Rayleigh numbers, Int. Commun. Heat Mass Tran. 38 (2011) 679–687.
[9] F. Xu, J.C. Patterson, C. Lei, Unsteady flow and heat transfer adjacent to the sidewall wall of a Differrentially heated cavity with a conducting and an adiabatic fin, Int. J. Heat Fluid Flow 32 (2011) 680–687.
[10] M. Yousaf, S. Usman, Natural convection heat transfer in a square cavity with sinusoidal roughness elements, Int. J. Heat Mass Tran. 90 (2015) 180–190.
[11] P. Chorin, F. Moreau, D. Saury, Heat transfer modification induced by a localized thermal Disturbance in a differentially-heated cavity, Int. J. Therm. Sci. 125 (2018) 101–110.
[12] M. Ohta, M. Akiyoshi, E. Obata, A numerical study on natural convective heat transfer of pseudo-plastic fluids in a square cavity, Numer. Heat Tran. A 41 (2002) 357–372.
[13] M. Lamsaadi, M. Naimi, M. Hasnaoui, M. Mamou, Natural convection in a tilted rectangular slot containing non-Newtonian power-law fluids and subject to a longitudinal thermal gradient, Numer. Heat Tran. A 50 (2006) 561–583.
[14] W.L. Barth, G.F. Carey, On a natural-convection benchmark problem in non-Newtonian fluids, Numer. Heat Tran. B 50 (2006) 193–216.
[15] M. Kaddiri, M. Naïmi, A. Raji, M. Hasnaoui, Rayleigh-Benard convection of non-Newtonian power law fluids temperature-dependent viscosity, ISRNThermodynamics 2012 (2012) 614712.
[16] O. Turan, A. Sachdeva, R.J. Poole, N. Chakraborty, Effects of aspect ratio onnatural convection of power-law fluids in rectangular enclosures with differentially heated vertical sidewalls, Int. J. Heat Mass Tran. 60 (2013) 722–738.
[17] M.A. Sheremet, T. Groşan, I. Pop, Steady-state free convection in rightangle porous trapezoidal cavity filled by a nanofluid: buongiorno's mathematical model, Eur. J. Mech. B Fluid 53 (2015) 241–250.
[18] R. Mahmood, S. Bilal, A.H. Majeed, I. khan, E.S.M. Sherif, A comparative analysis of flow features of Newtonian and power law material: a New configuration, J mater. Res. and Tech. 9 (2) (2020) 1978–1987.
[19] R. Mahmood, S. Bilal, A.H. Majeed, I. Khan, K.S. Nisar, Assessment of pseudo-plastic and dilatant materials flow in channel driven cavity: application of metallurgical processes, J mater. Res. and Tech. (2020) 3829–3837.
[20] R. Mahmood, S. Bilal, A.H. Majeed, I. Khan, K.S. Nisar, CFD analysis for characterization of non-linear power law material in a channel driven cavity with a square cylinder by measuring variation in drag and lift forces, J mater. Res. and Tech. (2020) 3838–3846.
[21] A.H. Majeed, F. Jarad, R. Mahmood, I. Saddique, Topological Characteristics of Obstacles and Nonlinear Rheological Fluid Flow in Presence of Insulated Fins: A Fluid Force Reduction Study, " Mathematical Problems in Engineering, 2021.
[22] A.H. Majeed, R. Mahmood, W.S. Abbasi, K. Usman, Numerical Computation of MHD Thermal Flow of Cross Model over an Elliptic Cylinder: Reduction of Forces via Thickness Ratio, " Mathematical Problems in Engineering, 2021.